Since January 2020 Elsevier has created a COVID-19 resource centre with free information in English and Mandarin on the novel coronavirus COVID-19. The COVID-19 resource centre is hosted on Elsevier Connect, the company's public news and information website.

CHAPTER 10

An optimized CNN based automated COVID-19 lung infection identification technique from C.T. images

R. Sharon Jebaleela[a], G. Rajakumar[a], T. Ananth Kumar[b], and S. Arunmozhiselvi[c]

[a]Francis Xavier Engineering College, Tirunelveli, India
[b]IFET College of Engineering, Gangarampalaiyam, India
[c]St. John the Baptist University, Mangochi, Malawi

1 Introduction

Coronavirus is a vast menace of viruses that can produce infection in every living organism. There are many coronaviruses from that; seven coronaviruses will cause the infection in human beings worldwide(Abdel-Basset, Chang, & Mohamed, 2020). Researchers are working harder than before. This rise in Cryptococcus volute infection because of COVID-19 outbreaks recently prompted them to find and control the rise of the infection (Wang, Horby, Hayden, & Gao, 2020). The Specific areas of investigation include surveillance of CoV2 mechanisms, research on the epidemiology of the virus, vaccines, and vulnerabilities that may occur during a pandemic, and the results of such research include looking into societal factors (Huang et al., 2020). Though there are seven coronaviruses, people get affected commonly by only four coronaviruses. The four common human being coronaviruses are 229E, NL63, OC43, and HKU1. Because these viruses cause coughing, Middle East Respiratory Syndrome(MERS), and life-threatening conditions like Severe Acute Respiratory Syndrome (SARS), the new Coronavirus is called COVID-19, known as Coronavirus Disease 2019, which is the same type of disease as found in monkeys infected with SARS (Abdel-Basset, Chang, & Nabeeh, 2021). Some viruses have a protective membrane, mainly made of macromolecules, which may allow the virus to survive better by offering nourishment for its single-celled moorings and enabling him to proliferate in cells (Ai et al., 2020). However, as

Novel AI and Data Science Advancements for Sustainability in the Era of COVID-19
https://doi.org/10.1016/B978-0-323-90054-6.00010-6

enzymes were then modified, this approach was no longer recognized, causing new viruses. During the 1970s, oncology was applied to curing cancers; at the moment was after 1980, antibodies were made that could recognize and fight the virus antigens on cancer cells.

Several viruses and their toxins are now discovered to target the unique chemistry of natural molecules that have been previously not selected as possible viruses or antibiotic drugs. While scientists and researchers have theorized that the random sequence of the polypeptide aided the escape, they have been unable to detect a particular domain-specific action that would lead to their whereabouts in the unknown polypeptide (namely, either finding "knowledge" or "discovering" domain-specific action"). Several known protein domains are required for this sequence and allow an expansion to the specific functional space to be found where it is possible to detect previously unidentified anti-work polypeptides (Shi et al., 2020). This service has facilitated search and will be used to develop and administer more designed systems that take advantage of software-assisted classifications for viral proteins to design and identify anti-viral treatments. During the experiments, scientists' earlier stages of preparation, some viruses were considered viable options. These microscopic organisms do enter cells at three stages of life and have three stages of development. These options to develop their viral antibodies: While conducting an experiment, three sorts of viruses may be thought of as possible hosts, each with three possible pathways that may help develop viral antibodies: anodyne macromolecules at different life stages (Jeyaranjani, Rajkumar, & Kumar, 2021). Those class A and cell class A viral molecules have three ways to gain and mix two ways to create new viruses. The assembly of essential cell components is needed for viral replication. With bacteria, the virus is just a part of the total composition of all things and cannot spread between people on its own. "Mobiles" power generation and "permeated by" gene material and/nucleic-protecting proteins do not yield substances and are therefore devoid of both power and capability for both protein production. Because of this, the viruses being smaller, the risk of illness from viruses is therefore lower. While the length of viruses is only 100-thousandth of a millimeter long, the length of bacteria is only 0.001% of a millimetric A large number of scientists doubt that this scientific community sees viruses as non-living entities (Pavithra, Rajmohan, Kumar, & Ramya, 2021). However, there is no widely accepted definition of "universal meaning" for the term "life" (none other than what a person wants to give it). The Coronavirus cannot replicate outside in the influence of other species. The virus can be treated using antibiotics to decrease its

genetic material and release it as much as possible; interferon contains interferon and envelope elements in a cell and protein (Fang et al., 2020). Each virus has a specific target cell, each of which has its own. This list of viruses includes a few that infect plants, many of which can affect animals, but other types of viruses affect humans. HIV, herpes, hepatitis, influenza, and mumps are responsible for human diseases, and yellow fever is a virus that causes these (Samuel, Pavithra, & Mohan, 2021). These drugs will be applied to all life forms: They will treat all viruses, but they will not affect the bacteria. Valero dismissed the idea of annihilating living organisms, which proved the point that he was making. Drug treatments, especially anti-viral, are frequently employed (Ye, Zhang, Wang, Huang, & Song, 2020). It is known as the "ViroStat," as it is known to be effective in preventing the proliferation of viruses because Although a pathogen causes the doctor's infection, in almost all cases, antibiotic resistance is also frequently found in the result (Bertram et al., 2021). Infection with HIV weakens the system, which allows bacteria to take advantage, causing more inflammation, which makes it difficult for the body to clear itself, while allowing the infection to fester and increase the amount of inflammation, allowing for more bacteria to invade the system (Dhiman, Chang, Kant Singh, & Shankar, 2021). The first name of the infectious disease was initially Novel Coronavirus Infected Pneumonia, and the virus was later renamed as the 2019-nCoV (Solomon et al., 2020). Then, on the 10th of September in the year 2021, the World Health Organization officially changed Corona Virus Disease 2020, which was released on Twitter, to Corona Virus Disease 2020 (Abitha, Babysha, Devisri, & Kumar, 2020). An epidemic of SARS-CoV-2 was brought about by the novel SARS-CoV-2 virus introduced in Wuhan, Hubei Province, during the year 2019. The contemporary epidemic is formally pervasive. After all, information about this virus (COVID-19) is rapidly spreading, and bookworms are advised to keep renovating themselves regularly in Fig. 1.

To help and prevent public health officials from health contamination, the reverse transcription-polymerase chain reaction (RT-PCR) is recommended (Balaji, Balamurugan, Kumar, Rajmohan, & Kumar, 2021). The instruments' insufficiency and great demands for analyzing the surroundings and reducing the high-speed and exact protecting of the distrusting matter. Additionally, RT-PCR checking tells of going through the large false, and the rate produced is negative (Ai et al., 2020). The necessary accompaniment is RT-PCR tests, and for the examination, radiological imaging techniques are used. The example is the radiogram, and C.T. scan determines the

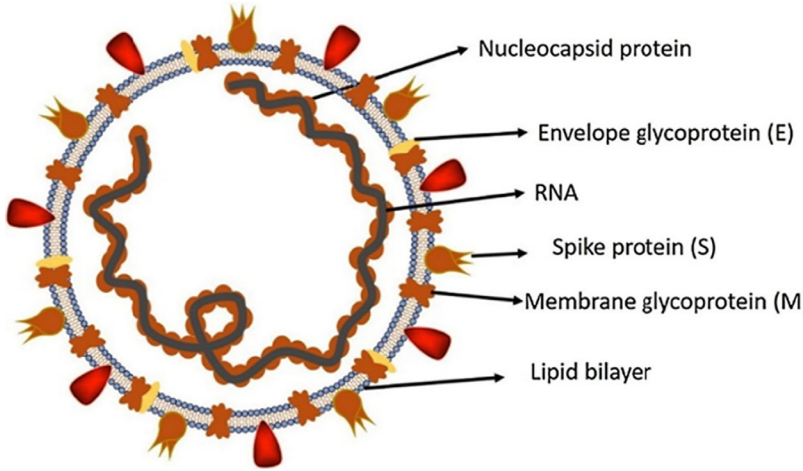

Fig. 1 A structure of respiratory syndrome (SARS) coronavirus.

benefits of both contemporary recognition, which contains the examined estimation, and the infection transformation appraisal (Hernigou et al., 2020) (Fig. 2). Fig. 2 denotes the transmission cycle of SARS CoV2.

Multilayer perceptrons (M-LP) have been miniaturized and trained on CNNs. The term "multilayer perceptrons" refers to a system with all neurons connected in a single layer of the network (Cohen et al., 2020). They are called "fully connected networks" by some authors. Therefore, the overall "connectedness" of these networks makes them prone to overfitting the data. Generally, any measure of magnitude is used in regularization; one of the popular approaches is to regularize the loss function by adding a multiplier Convolution method for expanding the meanings of patterns (Fan et al., 2020). The CNN's look for hierarchical data that allows them to constellate complex patterns. They look for more specific data that expands the scope of constellations by multiplying the meanings of built patterns using bigger and more intricate ones. In this way, CNNs are at the lower end of the scale on the connectedness and complexity scale. Biological processes were responsible for creating the connectomes in that several neurons, so that network patterns bear a resemblance to the organization of the visual cortex.

Receptive fields of individual neurons correspond to individual stimuli or stimuli in small areas within the receptive to a single area (Chowdhury et al., 2020). They have interwoven large receptive fields covering the entire visual field instead of being a point because of overlapping neural pathways.

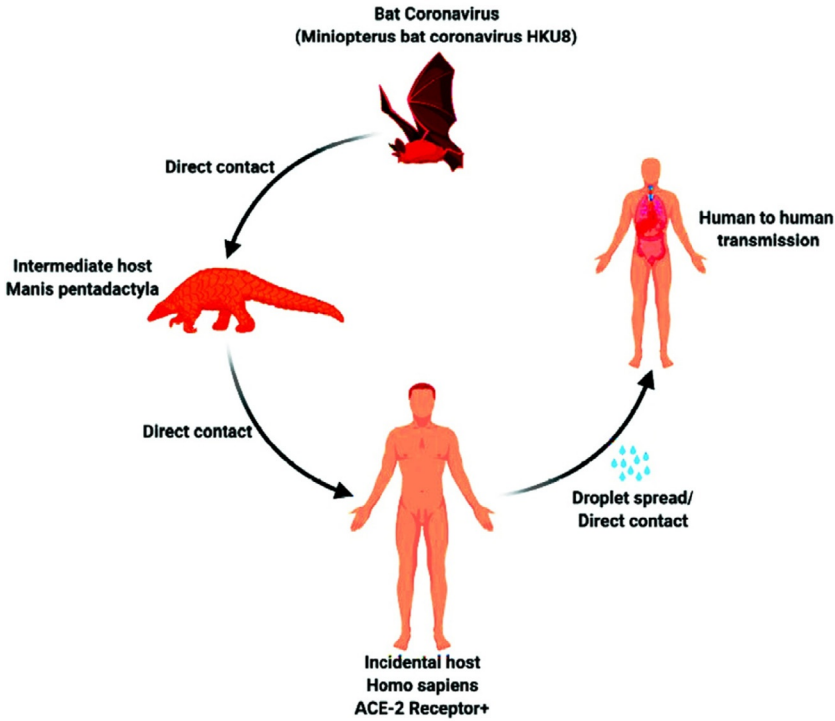

Fig. 2 Transmission cycle of SARS CoV2.

The CNN's are not nearly as much better than other image classification algorithms when processing image pre-to-intensive work (Kumar, John, & Kumar, 2020). The traditional algorithms allow for these, which means that the network has the hand-crafted filters expanded. Since prior knowledge and human effort were required for this design, this allowed the authors to avoid dealing with a myriad of issues that would have otherwise complicated matters.

Recently, patients infected with COVID-19 have been detected by deep learning systems via radiological imaging. For example, a COVID-Net was suggested to find COVID-19 in the patients by utilizing the chest radiography illustration. An anomaly detection model was designed to assist radiologists in evaluating the massive chest radiographs (Rajinikanth et al., 2020). In the C.T. scan, the position contemplation situated design to calculate the contamination possibility of COVID-19. A feebly directed expert system dependent on the operating scheme is progressed by utilizing a three-dimensional Computed Tomography batch in finding COVID-19.

This disease is found in the chest C.T. slices is a challenging responsibility and many other problems like (1) The significant difference in the appearance, extent, and the location of the diseases in the C.T. slices is challenging to find the infection. If the condensation is tiny or small, it will effortlessly produce the consequence in the negative rate, and the observation is false from the whole C.T. slice, (2) The differences between the inter-class are minor. They suggest COVID-19 Segmentation of Lung Infection by using deep Convolutional Neural Network from the chest C.T. images for leading the problem. The main desire functions are the experience in finding COVID-19 in the lung, and after discovering the infection, the doctor immediately removes the infected position and then precisely removes its relief as reported by the simple aspect. Hence, the content in which the field and the boundary are the two essential components and the difference between the other normal tissues and the lung's infection (Kumar, Selvi, Rajesh, Perumal, & Stalin, 2021).

The contribution of the proposed researches is; first, the input C.T. image is given, and in the subsequent process image is preprocessed by using the Grayscale image process, and the noises present in the image are removed. In the following process, the preprocessed image is given to the Convolutional Neural Network (CNN). In CNN, for Segmentation SqueezeNet, the feature extraction is used to extract the infections in the image and for classification Res-Net. The preprocessed image is given to the SqueezeNet Segmentation; it segments the lung separately from this chest C.T. image. The next process is feature extraction; the infections in segmented lung images are extracted. Finally, in this process, the classifier ResNet is used to classify the image, and it will compare with the already trained images and produce the result as COVID-19 positive or negative.

2 Literature review

The Authors proposed an automatic way that enables the robust Segmentation of the infected lungs, which have the infections joined with the parenchyma, and the respiratory variation antiquity influences them in a *Mycobacterium tuberculosis* contamination pattern. Lung segmentation is the step before biomarker extraction (Gokulan, Narmadha, Pavithra, Rajmohan, & Ananthkumar, 2020). The fundamental ways to separate fine bronchi tissue and the air passage tree are then replaced by the rejection of the linty borders (Keshani, Azimifar, Tajeripour, & Boostani, 2013). The achievement was related to the separation is obtained by using: (1) a half operating

device and (2) a beginning which depends on linty accordance. The accord apportionment, which results from the generality of voting by the three adept clarifications, is regarded through ground control. The authors proposed an information-directed pattern, described the Central Focused Convolutional Neural Networks (CF-CNN), to separate the lung clot from the heterogeneous X-ray scan (Wang et al., 2017). This methodology is used to merge the significant two observation: (1) the suggested pattern takes the disparate position in the clot delicate characteristics in a couple of the three dimensions and the two-dimension C.T. images repeatedly, (2) once ordering the depiction voxel, then the impacts with the acquaintance of the voxels may differ as respected by the epidemic of the computative area (Jin, Xu, Tang, Harrison, & Mollura, 2018). It is an incident suggesting a novel central pooling layer that retains more data in a voxel patch center, and then it is replaced by a multi-scale patch learning approach. Besides, a loaded experience is used to assist the instruction pattern, and the instructed models are chosen based on the standard of the apportionment problem.

Volume changes from computed tomography (C.T.) and longitudinal ability to track tumor growth from the computed tomography (C.T.) are required to monitor tumor response. In other words, in developing two residually connected networks (INC) and dense network (DENSE) formulations, we designed INC and DENS and INC (Srimathi & Ananthkumar, 2020). This set of unites detection and segmentation features connect multiple feature levels at once or join different detection levels to operate across tumor recognition. In essence, the MRRN is two different; the multi-resolution neural network (MRRN) used in incremental/dense networks is an upgrade of the existing single-resolution neural. (for sparse MRRN) (for the incremental MRRN). Another aspect of combination stream refinement involves refining features in each residual layer after that is achieved (Rajmohan, Kumar, Pavithra, & Sandhya, 2020). There are many issues with getting disease models that work with imaging and imaging measurement during treatment and monitoring treatment. Most models are created by accumulating lots of data annotated with previously known markers to detect small entities (Zhao et al., 2021). The approach's potential to be fruitful in terms of knowledge and greater simplicity may be brought to bear against a bit of annotation effort. The vocabulary and autonomous classifiers' vocabulary hereto search for anomalies in imaging data to classifiers to handle the data alone. An extension of a deep convolution network can learn a manifold of anatomical variations in tandem with a novel scoring algorithm. It is also based on representing the 3D shape of the image space

and the latent space. The model is extended to new image data and assigns a score to each one to determine how well the anomaly fits into the distribution.

The medical image segmentation technology presented in this paper makes use of a novel, more robust architecture. Deep skip routing like this can be considered a sophisticated translation circuitry for depth instruction encoding because the encoder and decoder work in tandem and deep routes. As the complexity between the encoder network's feature maps and the workflows is decreased, the new skip pathways were employed to make the systems more similar. An argument would be made for better exploration and exploitation by the feature extractor and expand network when the decoder and the feature extractor/expand network are semantically similar. Its comparison with U-Net and comprehensive U-Net architectures for different segmentation techniques has shown it successful: nodule segmentation in low-dose C.T., nucleation in microscopy images, and polyplastic colon scans have been successfully carried out (Zhou, Siddiquee, Tajbakhsh, & Liang, 2018). These three main modules (of the three) can be found in the Content Expansion module (CENet): a feature module, a context extractor module, and a feature expander. The newly pre-trained ResNet block is used as an extractor of the fixed features Also called atrous convolution expansion (as we were before), the new Atrous block and residual pooling (as the phrase implies) have just been proposed together make up the base of the Dense Context Extraction (D.E.) module. The project's goal is to expand the reach of the CEDAXI System to both medical imaging tasks. Because it out shares better than the original U-Net method and other state-of-of-the-the-the-art methods for identifying the different stages of eye diseases such as optic disc-visual, cell layer segmentation, retinal layer, and lung segmentation, it excels in vessel contour delineation.

3 Proposed system

The COVID-19 has the main diagnostics to be done in the Lungs as it is the vital cause of infection slows down the SPO2 level. The infection made in the bilateral walls of the Lungs makes suffer the person with COVID-19.

The easy diagnosis of the infections helps the doctors to treat the COVID-19 patients easier. There are many deep learning concepts to diagnose infections. The advanced Segmentation technique detects a novel coronavirus in the lung by using Deep Residual Network (Resnet50).

It is suggested here to find the affected portion in the chest X-ray scan inevitably. SqueezeNet CNN (Convolutional Neural Network) is used for lung segmentation. After Segmentation, extract the features and advance the recognition of the affected area in the lungs by using the residual network Technique. Residual network technique is first analyzed and then applied in the process of the conclusion of COVID-19, for example, evaluating the affected regions and checking the longitudinal infection changes. Fig. 3 shows the architecture of the proposed system.

3.1 Pre-processing

While arranging coherent cacophony constraint strainers, it will have a batch of effort. The pre-treating or straining process is used for decreasing the deterioration, which is analogous to the cacophony. Like the shadow on the input depiction, the cacophony is extracted by utilizing the pre-treating strainers like the average strainers. Here, extracting the cacophony from the input is a crucial stage, and it is obligatory for intensifying lung depiction grade then makes the attribute abstraction intrinsic more excellent dependable on the advance of comprehensive and small input depiction.

3.2 Lung segmentation

The Proposed work is implemented with the CNN-based SqueezeNet method for lung segmentation which includes a deep Convolutional Neural Network (CNN). The model contains a relatively small amount of parameters. To achieve the correct AlexNet level in the ImageNet dataset and it will contain 50 × fewer parameters.

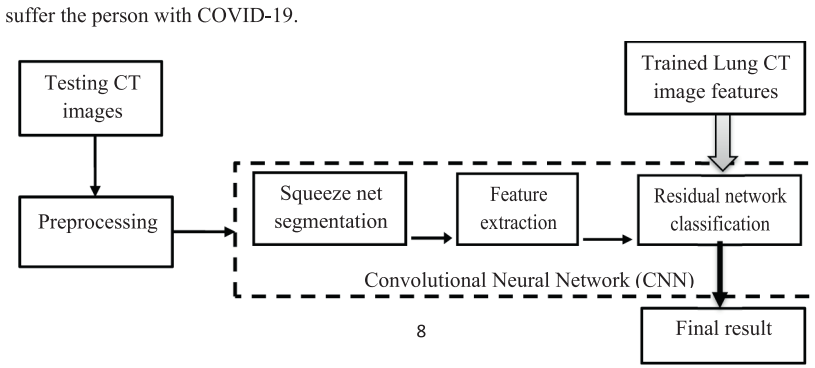

Fig. 3 Proposed block diagram.

Three advantages of small CNN architectures:

- CNN needs only little contact beyond the servers in the course of apportions coaching.
- CNN needs small bandwidth to convey the recent pattern in the cloud (Suresh Kumar, Radha Mani, Sundaresan, & Ananth Kumar, 2021).
- It is more feasible to deploy on customized hardware with limited memory.

(a) SqueezeNet architecture explanation

It gives three fundamental strategies for decreasing the area of the parameter while increasing reliability. Fig. 4 shows the diagram of the 3×3 filter, and Fig. 5 shows the diagram of the 1×1 filter.

Strategy 1

- Strategy 1 is to generate the network lesser by following 3×3 filters with 1×1 filters.
- Conventional 3×3 replaced by 1×1 convolution filters.
- 1×1 filters have $9\times$ lesser parameters than 3×3 filters.
- Difference between 3×3 filters and 1×1 filters.

3×3 filters

- Larger special receptive field.
- They are imprisoning the computative data of the pixels adjacent to each other.

1×1 filters

- Looks at one pixel at the time.
- Captures relationships amongst its channels.
- Equivalent to a fully connected layer along the channel dimension.

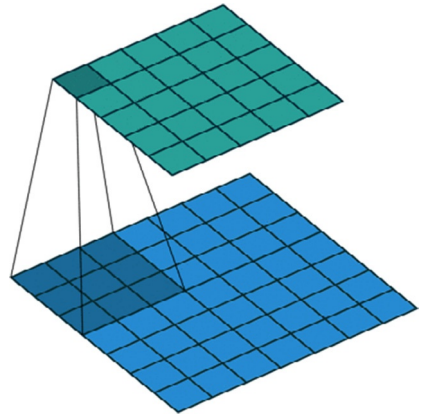

Fig. 4 3×3 filters.

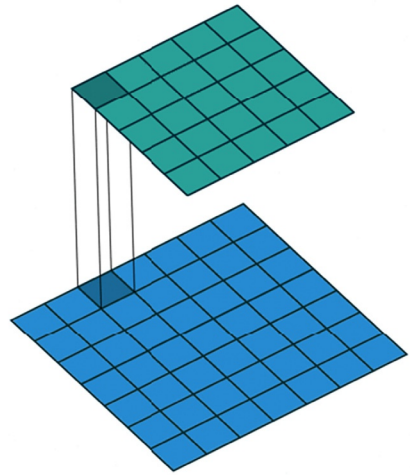

Fig. 5 1×1 filters.

Strategy 2

Strategy 2 is used to lessen the total inputs in abide of 3×3 filters.

- Fewer inputs to Conv layers result in fewer parameters.
- It is achieved by using only 1×1 filters before the 3×3 Conv layers.
- It is called the squeeze layer (description in next section).
- Total parameters in a 3×3 Conv layer = (total input channels) (total filters) (3×3).

Strategy 3

Strategy 3 is used in the down-sample late, which are in the grid because of that the convolution layers will retain more number of the awaking maps.

- It mostly makes a smaller number of parameters and maximizes accuracy.
- Delaying down sampling late in the network creates more extensive activation of feature maps.
- Leaving from more traditional architectures like the VGG network that use early down sampling.
- Large activation maps result in a higher classification accuracy given the same number of parameters.

(b) Fire Module

In the fire module, there is various squeeze convolution layer, and it consists of only 1×1 filters, which provide it into an expand layer

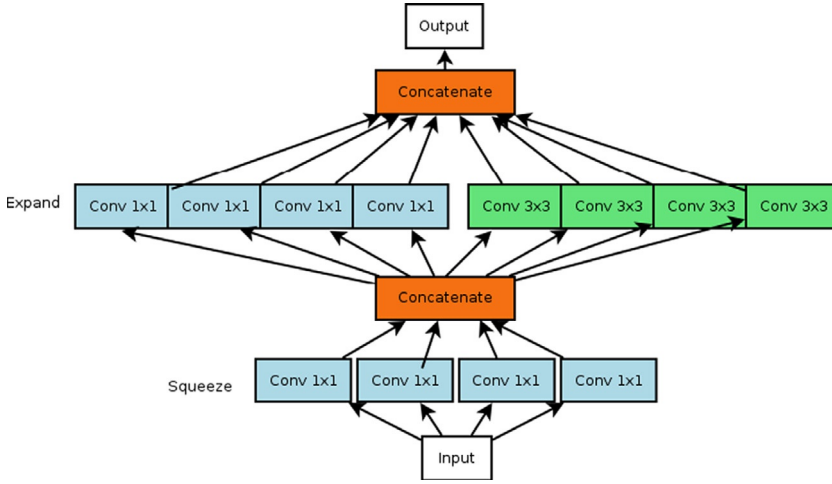

Fig. 6 Fire module.

consisting of a mixture of 1×1 and 3×3 convolution filters, which is shown in Fig. 6. Here, three different tunable dimensions (hyper-parameters) are in a Fire module: $s1 \times 1$, $e1 \times 1$, and $e3 \times 3$. The hyper-parameters (i.e., $s1 \times 1$) in a fire module has many filters which are utilized in the layer, which is called the squeeze layer (all 1×1) has a total of 1×1 in expanding layer then here in this stage, $e3 \times 3$ is the total of 3×3 filters which is also used in expanding layer. Here, the Fire module is used and deposited in the s1x1which must be smaller than $(e1x1 + e3 \times 3)$. Therefore, the squeeze layer supports restricting the total input channels of the 3×3 filters by using Strategy 2.

(c) SqueezeNet Architecture

The SqueezeNet Convolutional Neural Network (CNN) architecture, illustrated in Fig. 7 in which the SqueezeNet begins beside a standalone convolutional layer (i.e., conv1), which will come after with a totally of 8 Fire modules (i.e., fire2–9) and it will end with a final convolutional layer (i.e., conv10). Here, total filters slowly rise in each fire module, which starts close to finishing the network. The max pool with a stride of 2 below these layers in SqueezeNet: conv1, fire4, fire8, and conv10; these layers are almost late placements of the pooling are in each of the Strategy 3.

Layers breakdown has eleven layers:

- The first layer is the regular Convolution layer.
- The second layer up to the ninth layer is the Fire module layer (squeeze + expand layer).

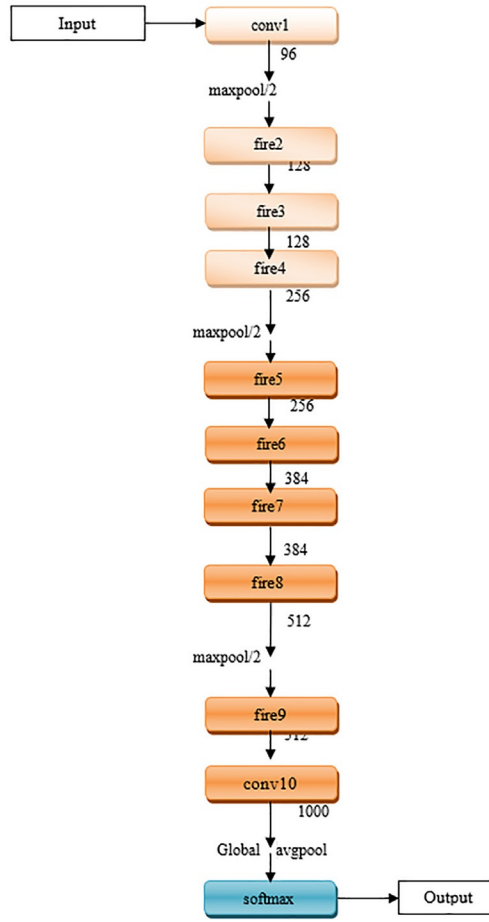

Fig. 7 SqueezeNet architecture.

- The tenth layer is also the regular convolution layer.
- The eleventh layer is the Softmax layer.

3.3 Feature extraction

Feature extraction is the procedure of planning a current Convolutional Neural Network design which is a very monotonous step, and it needs the large capacity of the information and the assets during the implementation. The pre-coached designs like AlexNet will assimilate during the transfer learning. Here, AlexNet works are dependent on the architecture of CNN for transfer learning. Initially, the pre-coached AlexNet designs along the ImageNet dataset force are extracted for the feature extraction along the

ImageNet dataset with the comprehend filters of the Convolutional Neural Network architectures; by using these steps, feature coordinate is collected. The pre-coached CNN pattern has the initial category of layers consisting of the least number of features with crucial complementary details similar to the edges. Finally, completely connected layers of the pre-coached network are extracted. The utterly connected layer neuron is now added to the head of the convolutional layers. They are used for gathering the removed features from the convolutional layers. Finally, the inspection of the various completely connected layers has an adequate perception as the decision.

3.4 Residual network (ResNet) classification

ResNet has been designed to create networks that are ultra-deep. ResNet falls under the deep learning category. ResNet is used not only for deep learning but also for more applications like natural language processing. ResNet was designed with several layers of nodes, such as making 34th layer, 50th layer, 101st layer, 152nd layer, and even 1202nd layer of nodes with different layers. ResNet50, the famous convolutional network, is the network with 49 convolutional layers and one fully-connected layer at the network's bottom. To get the total weight and MAC to the entire network, we need 25.5 million pounds and 3.9 million pounds. The ResNet architecture is shown as the basic block diagram, as seen in the colorful illustration in Fig. 8.

Residual Network (ResNet) is a conventional feed-forward lattice that has the remaining connection. The residual layer's output is explained by the bases in the outputs by the precursory layer, explained as $xl-1$. $F(xl-1)$ is the output behind executing different performances. For example, the convolution with dissimilar sizes of the filters, Batch Normalization (B.N.) is pursued by the stimulation responsibility, like a ReLU $xl-1$. The accomplishment output of the residual of the unit is xl that the following equation might express as,

$$xl = F(xl-1) + xl - 1 \tag{1}$$

Residual network (ResNet) contains lots of the fundamental residual blocks. The functions present in the residual block could be differed based on the non-identical structural design of the residual networks. The residual network's comprehensive description was suggested, and then the surrogate advanced residual network perspective is called as the accumulated residual metamorphose was produced.

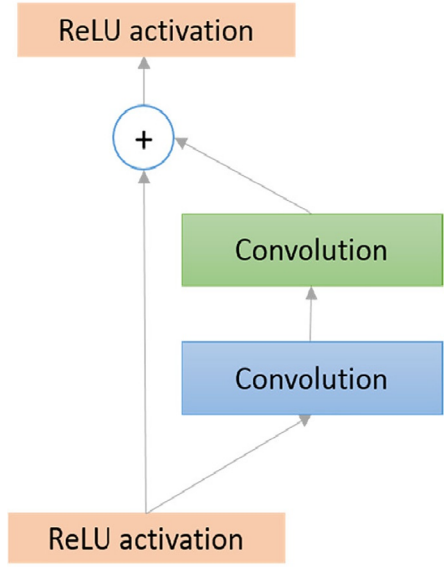

Fig. 8 Block diagram of the ResNet architecture.

Newly, some interchangeable alternative of the residual designs is initiated, and it depends on the Residual Network architecture. Furthermore, various developed architectures are integrated by the establishment of the Residual units. The fundamental imaginary illustration of the Inception Residual unit is exhibited in the following Fig. 9.

4 Simulation results and discussion

As the validation of the Proposed work, the input is given, and the parameters measured play a significant role. Some sample data set has been used as input. The simulation has been resulted using MATLAB based on the parameter like high precision, Dice scores, specificity, and precision. The following Fig. 10 represents the sample C.T. lungs image tested with this proposed work.

The RGB image is converted to a Gray image. The input images consume more memory to process. Therefore the image is converted into grayscale where only one band will represent the pixel value that varied from 0 to 255. The following Fig. 11 shows the grayscale image.

The preprocessed image is the extraction of the portion of the lung from the X-ray scan input along with the other pixels are given as "0." In the

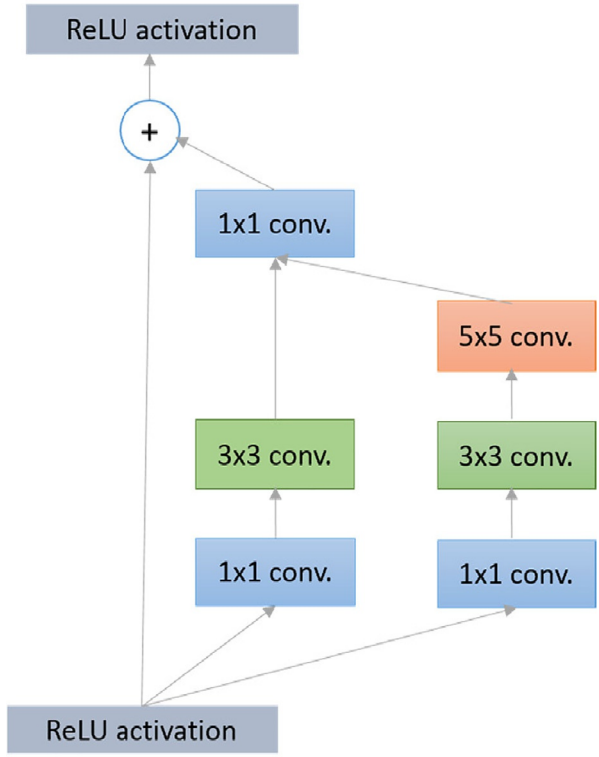

Fig. 9 Block diagram for inception residual unit.

preprocessed image, the image contrast is improved, and the noises are removed. After grayscale conversion, improve the contrast of the image by using an average filter. The following Fig. 12 represents the pre-processing image.

After pre-processing, the image is contoured. The process of the initial contour is used to contour the lungs separately in the C.T. image. The following Fig. 13 represents the Initial contour.

After contouring, the image has been iterated. The iteration stage is the operation of manipulating individual components in the digital structure. In order to operate all of the pixels, we need to be able to visit all the rows and the columns entirely in the image. The following Fig. 14 represents the iteration image.

The final boundary mask image will convert the segmentation gray image to the black and white image. This process separates the lung image from the C.T. image. The following Fig. 15 represents the final boundary mask.

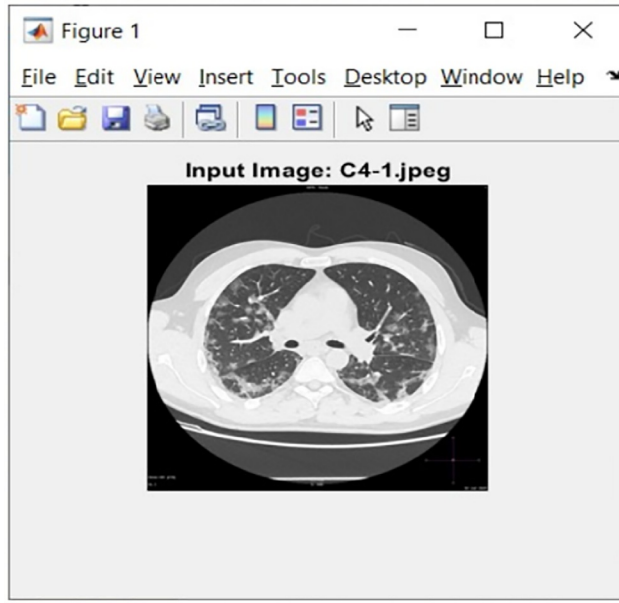

Fig. 10 Input image.

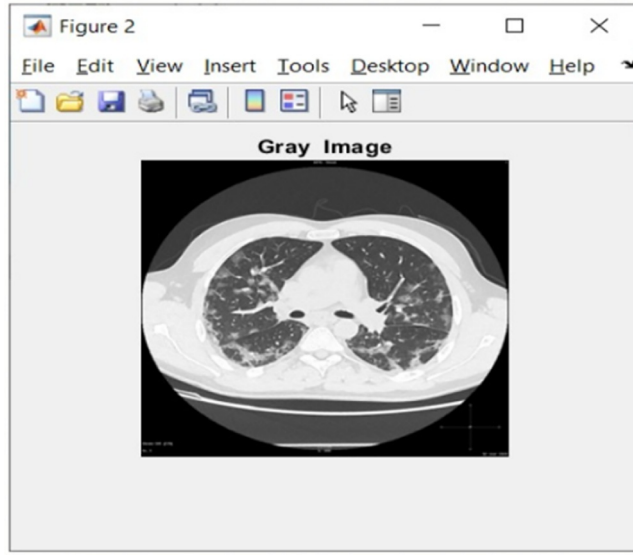

Fig. 11 Grayscale image.

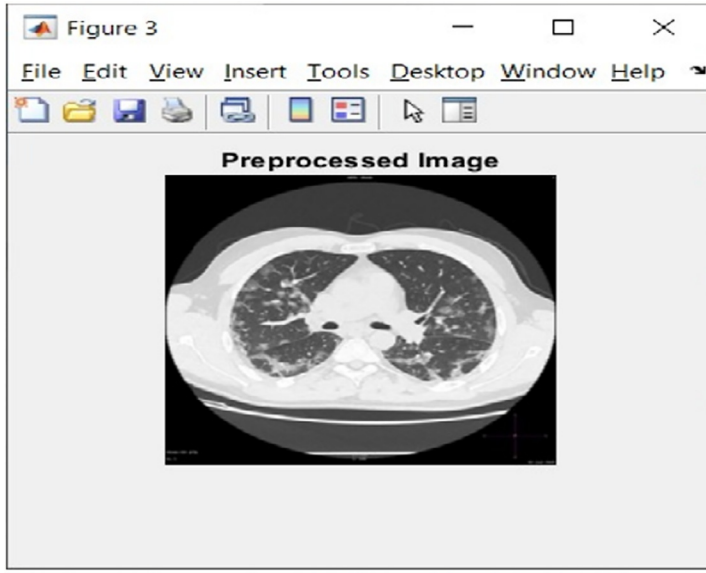

Fig. 12 Pre-processed image.

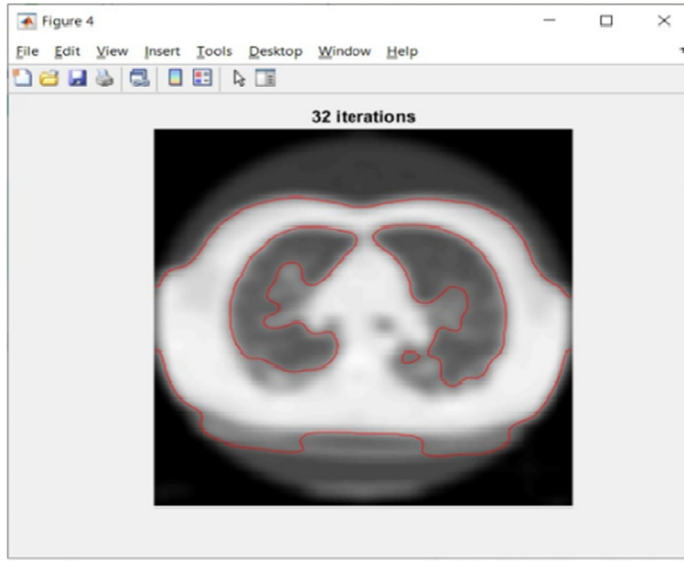

Fig. 13 Image at the initial contour.

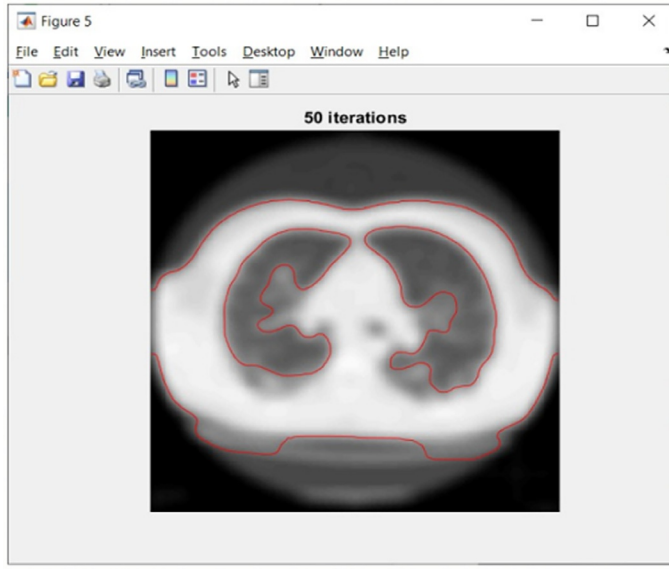

Fig. 14 Iteration image.

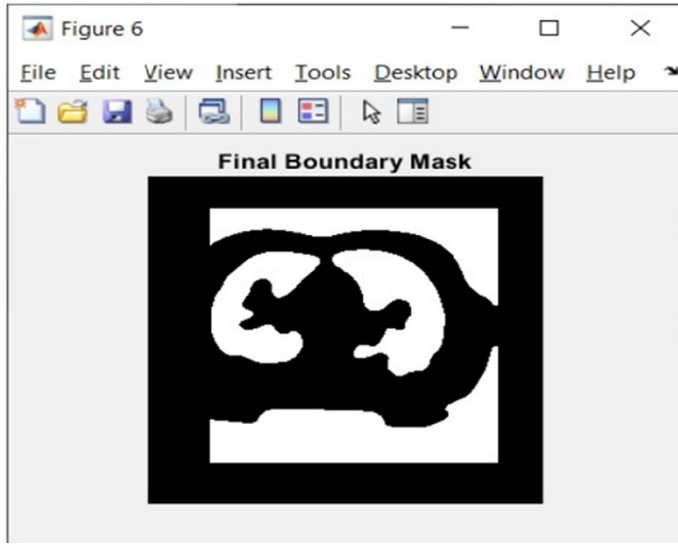

Fig. 15 Final boundary mask image.

After the final boundary mask image process, the Segmentation takes place by SqueezeNet CNN. In this segmentation process, the infected region is segmented from the lungs in the image by SqueezeNet Segmentation. The following Fig. 16 represents the Segmentation of the mask image.

After Segmentation, the layer processing step compares the image to the already trained C.T. images and produces the result. CNN-based classification is processed to classify whether the image is positive or negative. The following Fig. 17 shows the first convolutional layer's weights.

After the process of the image by Convolutional Network, the result is displayed. The result shows whether COVID-19 is positive or negative. Fig. 18 shows the final predicted output of the system.

Formula used for performance evaluation:

$$\text{Sensitivity} = \text{TP}/\text{P} \tag{2}$$

$$\text{Specificity} = \text{TN}/\text{N} \tag{3}$$

$$\text{Precision} = \text{TP}/(\text{TP} + \text{FP}) \tag{4}$$

$$\text{Accuracy} = (\text{TP} + \text{TN})/(\text{P} + \text{N}) \tag{5}$$

Dice score shall be calculated from the below formula,

$$\text{Dice score} = 2 \times \text{number of true positives}/(2 \times \text{number of true positives} + \text{number of false positives}) + \text{number of false negatives} \tag{6}$$

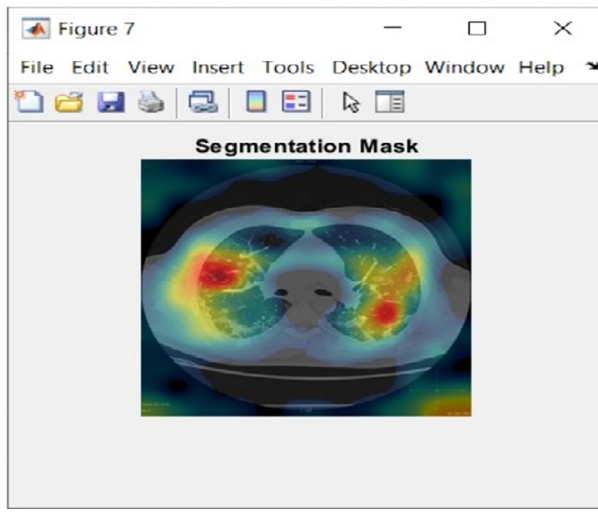

Fig. 16 Segmentation mask image.

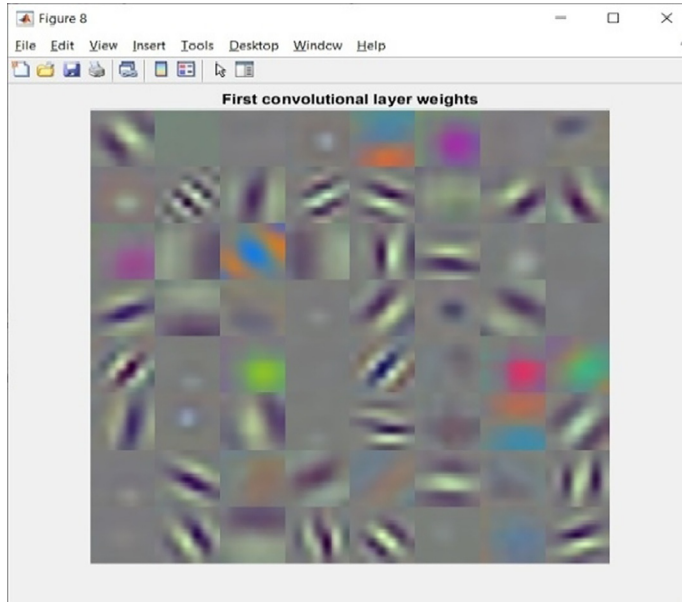

Fig. 17 CNN processing image large weights.

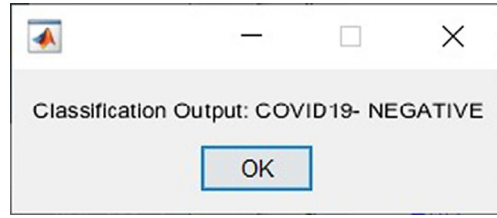

Fig. 18 Classification output.

Where,
P—condition positive
N—condition negative
TP—True positive
TN—True negative
FP—false positive
FN—false negative

Here, P denotes the number of real positive cases in the data. N represents the number of real negative cases in the data. TP is equivalent with hit. TN denotes equivalent with correct rejection. FP represents equivalent with underestimation and FN denotes equivalent with overestimation.

Table 1 Performance evaluation.

Model	Dice	Sen.	Spec.	Prec.	Accu.
U-Net	0.309	0.676	0.837	0.267	91.7
Attention-UNet	0.468	0.725	0.934	0.393	92.9
Gated-UNet	0.445	0.673	0.958	0.376	93.3
Dense-UNet	0.412	0.609	0.979	0.417	94.8
U-Net++	0.447	0.876	0.927	0.367	92.1
Squeeze-Net	0.578	0.871	0.977	0.503	97.8
Res-Net(proposed)	0.599	0.867	0.979	0.517	98.2

Table 1 shows the performance comparison of different existing methods with the proposed method. The specificity of the proposed method is 0.977 out of 1. The accuracy of the result produced from Fig. 17 is 98.2%. The proposed method accuracy has been ensured based on high precision, specificity, and Dice scores, even though the sensitivity is slightly low compared with existing methods. The specificity and precision are directly proportional to accuracy. Table 1 performance evaluation parameters rounding the scale value is 1, except accuracy mentioned in the percentage.

5 Conclusion

Thus an automatic detection of coronavirus 2019 infection in the lung by using segmentation process from C.T. images has been simulated. The named deep residual network in Convolutional Neural Network (CNN) is used and the definite reverse attention and the distinct edge attention for developing the recognition of the affected area in the lung are applied, with the help of chest C.T. slices. This structure holds admirable possible which can be sought during the evaluation in detecting COVID-19, for example, computing the affected area, observing the longitudinal infection difference, and aggregation disguising transforming. Datasets were performed as input data to the SqueezeNet network using the image processing techniques. The network achieved is of higher accuracy. Thus the proposed model can recognize the recipients with less power and compare the lung and the affected area of the normal tissues. The Simulation results revealed that the Accuracy had attained it peak compared to the existing models.

References

Abdel-Basset, M., Chang, V., & Mohamed, R. (2020). HSMA_WOA: A hybrid novel slime mould algorithm with whale optimization algorithm for tackling the image segmentation problem of chest X-ray images. *Applied Soft Computing*, *95*, 106642.

Abdel-Basset, M., Chang, V., & Nabeeh, N. A. (2021). An intelligent framework using disruptive technologies for COVID-19 analysis. *Technological Forecasting and Social Change*, *163*, 120431.

Abitha, N., Babysha, P., Devisri, S., & Kumar, P. (2020). Application of DL/ML in diagnosis in medical imaging. *Journal on Intelligent Systems & Robotics Insights & Transformations*, *4*(1) (ISSN: 2581-5636 (online)).

Ai, T., Yang, Z., Hou, H., Zhan, C., Chen, C., Lv, W., et al. (2020). Correlation of chest C.T. and RT-PCR testing for coronavirus disease 2019 (COVID-19) in China: A report of 1014 cases. *Radiology*, *296*(2), E32–E40.

Balaji, S., Balamurugan, B., Kumar, T. A., Rajmohan, R., & Kumar, P. P. (2021). A brief survey on AI-based face mask detection systems for public places. *Irish Interdisciplinary Journal of Science & Research (IIJSR)*, *5*(1), 108–117.

Bertram, K. M., Truong, N. R., Smith, J. B., Kim, M., Sandgren, K. J., Feng, K. L., et al. (2021). Herpes simplex virus type 1 infects Langerhans cells and the novel epidermal dendritic cell, Epi-cDC2s, via different entry pathways. *PLoS Pathogens*, *17*(4), e1009536.

Chowdhury, M. E., Rahman, T., Khandakar, A., Mazhar, R., Kadir, M. A., Mahbub, Z. B., et al. (2020). Can AI help in screening viral and COVID-19 pneumonia? *IEEE Access*, *8*, 132665–132676.

Cohen, J. P., Morrison, P., Dao, L., Roth, K., Duong, T. Q., & Ghassemi, M. (2020). *Covid-19 image data collection: Prospective predictions are the future*. arXiv preprint arXiv:2006.11988.

Dhiman, G., Chang, V., Kant Singh, K., & Shankar, A. (2021). Adopt: Automatic deep learning and optimization-based approach for detection of novel coronavirus covid-19 disease using x-ray images. *Journal of Biomolecular Structure and Dynamics*, 1–13. https://doi.org/10.1080/07391102.2021.1875049.

Fan, D. P., Zhou, T., Ji, G. P., Zhou, Y., Chen, G., Fu, H., et al. (2020). Inf-net: Automatic covid-19 lung infection segmentation from ct images. *IEEE Transactions on Medical Imaging*, *39*(8), 2626–2637.

Fang, Y., Zhang, H., Xie, J., Lin, M., Ying, L., Pang, P., et al. (2020). Sensitivity of chest C.T. for COVID-19: Comparison to RT-PCR. *Radiology*, *296*(2), E115–E117.

Gokulan, S., Narmadha, S., Pavithra, M., Rajmohan, R., & Ananthkumar, T. (2020, July). Determination of various deep learning parameter for sleep disorder. In *2020 international conference on system, computation, automation and networking (ICSCAN)* (pp. 1–6). IEEE.

Hernigou, J., Cornil, F., Poignard, A., El Bouchaibi, S., Mani, J., Naouri, J. F., et al. (2020). Thoracic computerised tomography scans in one hundred eighteen orthopaedic patients during the COVID-19 pandemic: Identification of chest lesions; added values; help in managing patients; burden on the computerised tomography scan department. *International Orthopaedics*, *44*(8), 1571–1580.

Huang, C., Wang, Y., Li, X., Ren, L., Zhao, J., Hu, Y., et al. (2020). Clinical features of patients infected with 2019 novel coronavirus in Wuhan, China. *The Lancet*, *395*(10223), 497–506.

Jeyaranjani, J., Rajkumar, T. D., & Kumar, T. A. (2021). Coronary heart disease diagnosis using the efficient ANN model. *Materials Today: Proceedings*, *1*, 1–5. https://doi.org/10.1016/j.matpr.2021.01.257.

Jin, D., Xu, Z., Tang, Y., Harrison, A. P., & Mollura, D. J. (2018, September). CT-realistic lung nodule simulation from 3D conditional generative adversarial networks for robust

lung segmentation. In *International conference on medical image computing and computer-assisted intervention* (pp. 732–740). Cham: Springer.
Keshani, M., Azimifar, Z., Tajeripour, F., & Boostani, R. (2013). Lung nodule segmentation and recognition using SVM classifier and active contour modeling: A complete intelligent system. *Computers in Biology and Medicine*, *43*(4), 287–300.
Kumar, T. A., John, A., & Kumar, C. R. (2020). *2 IoT technology and applications. Internet of Things* (p. 43). Germany: De Gruyt.
Kumar, T. A., Selvi, S. A., Rajesh, R. S., Perumal, P. S., & Stalin, J. (2021). Limos—Live patient monitoring system. In *Handbook of artificial intelligence in biomedical engineering* (pp. 311–330). Apple Academic Press.
Pavithra, M., Rajmohan, R., Kumar, T. A., & Ramya, R. (2021). Prediction and classification of breast cancer using discriminative learning models and techniques. In *Machine vision inspection systems, volume 2: Machine learning-based approaches* (pp. 241–262). India: Scrivener Publishing LLC.
Rajinikanth, V., Dey, N., Raj, A. N. J., Hassanien, A. E., Santosh, K. C., & Raja, N. (2020). *Harmony-search and otsu based system for coronavirus disease (COVID-19) detection using lung C.T. scan images*. arXiv preprint arXiv:2004.03431.
Rajmohan, R., Kumar, T. A., Pavithra, M., & Sandhya, S. G. (2020). 11 Blockchain. In *177. Blockchain technology: Fundamentals, applications, and case studies*. United States: CRC Press.
Samuel, T. A., Pavithra, M., & Mohan, R. R. (2021). LIFI-based radiation-free monitoring and transmission device for hospitals/public places. In *Multimedia and sensory input for augmented, mixed, and virtual reality* (pp. 195–205). IGI Global.
Shi, F., Wang, J., Shi, J., Wu, Z., Wang, Q., Tang, Z., et al. (2020). Review of artificial intelligence techniques in imaging data acquisition, segmentation and diagnosis for covid-19. *IEEE Reviews in Biomedical Engineering*, *14*, 4–15. 2021 https://doi.org/10.1109/RBME.2020.2987975.
Solomon, M. D., McNulty, E. J., Rana, J. S., Leong, T. K., Lee, C., Sung, S. H., et al. (2020). The Covid-19 pandemic and the incidence of acute myocardial infarction. *New England Journal of Medicine*, *383*(7), 691–693.
Srimathi, B., & Ananthkumar, T. (2020). Li-Fi based automated patient healthcare monitoring system. *Indian Journal of Public Health Research & Development*, *11*(2), 393–398.
Suresh Kumar, K., Radha Mani, A. S., Sundaresan, S., & Ananth Kumar, T. (2021). Modeling of VANET for future generation transportation system through edge/fog/cloud computing powered by 6G. In *Cloud and IoT-based vehicular ad hoc networks* (pp. 105–124). United States: : John Wiley & Sons, Inc.
Wang, C., Horby, P. W., Hayden, F. G., & Gao, G. F. (2020). A novel coronavirus outbreak of global health concern. *The Lancet*, *395*(10223), 470–473.
Wang, S., Zhou, M., Liu, Z., Liu, Z., Gu, D., Zang, Y., et al. (2017). Central focused convolutional neural networks: Developing a data-driven model for lung nodule segmentation. *Medical Image Analysis*, *40*, 172–183.
Ye, Z., Zhang, Y., Wang, Y., Huang, Z., & Song, B. (2020). Chest CT manifestations of new coronavirus disease 2019 (COVID-19): A pictorial review. *European Radiology*, *30*(8), 4381–4389.
Zhao, S., Huang, Q., Tang, Y., Yao, X., Yang, J., Ding, G., et al. (2021). *Computational emotion analysis from images: Recent advances and future directions*. arXiv preprint arXiv:2103.10798.
Zhou, Z., Siddiquee, M. M. R., Tajbakhsh, N., & Liang, J. (2018). Unet++: A nested u-net architecture for medical image segmentation. In *Deep learning in medical image analysis and multimodal learning for clinical decision support* (pp. 3–11). Cham: Springer.